NASA Technical Memorandum 72855

Flight-Measured Pressure Characteristics of Aft-Facing Steps in High Reynolds Number Flow at Mach Numbers of 2.20, 2.50, and 2.80 and Comparison With Other Data

Sheryll Goecke Powers

MAY 1978

NASA

NASA Technical Memorandum 72855

Flight-Measured Pressure Characteristics of Aft-Facing Steps in High Reynolds Number Flow at Mach Numbers of 2.20, 2.50, and 2.80 and Comparison With Other Data

Sheryll Goecke Powers
Dryden Flight Research Center
Edwards, California

National Aeronautics
and Space Administration

**Scientific and Technical
Information Office**

1978

FLIGHT-MEASURED PRESSURE CHARACTERISTICS OF AFT-FACING STEPS IN HIGH REYNOLDS NUMBER FLOW AT MACH NUMBERS OF 2.20, 2.50, AND 2.80 AND COMPARISON WITH OTHER DATA

Sheryll Goecke Powers
Dryden Flight Research Center

INTRODUCTION

Surface discontinuities formed by the trailing edges of wings and panels and other aft-facing discontinuities are known to be a source of drag for an airplane. The theories and models developed in the 1950's for base pressures in supersonic turbulent flow were usually simplified by assuming the initial or approaching boundary layer thickness to be zero or approaching zero (Korst's theory, ref. 1, and Chapman's model, ref. 2). Correlations were developed from experimental data to account for the effect of the initial boundary layer thickness on the base pressure for a given Mach number. For example, in the early 1950's, Chapman, Wimbrow, and Kester (ref. 3) established a relationship between base pressure ratio and base thickness, Reynolds number, and length of the body upstream of the base for Mach numbers ranging from 1.5 to 3.1, and in the mid-1960's, Hastings (ref. 4) showed a relationship between base pressure ratio and the ratio of momentum thickness to step height for Mach numbers ranging from 1.56 to 3.10. Hasting's data covered a wide range of ratios of momentum thickness to step height (from near zero to approximately 2) but were for a relatively thin initial boundary layer (a momentum thickness of less than 0.05 centimeter (0.02 inch)). Two experiments with thick boundary layers were conducted in the mid-1960's and early 1970's (refs. 5 and 6, respectively). The data of reference 5, for which the momentum thickness was approximately 0.76 centimeter (0.30 inch), were obtained for two step heights at a Mach number of 2.8. The data of reference 6, for which the momentum thickness was approximately 1.27 centimeters (0.50 inch), were obtained for one step height for a Mach number range of 0.4 to 2.5. At Mach numbers of 2.0 and above, the base pressure ratios for the thin boundary layer data of reference 4 differed from those for the thick boundary layer data of references 5 and 6. For ratios of momentum thickness to step height of approximately 1, both the thick boundary layer studies had lower base pressure ratios (more drag) than the thin boundary layer study, and the disagreement became greater with increasing Mach

number. Because of the limited amount of thick boundary layer data available, further study was needed to determine how and why the curves for base pressure ratio as a function of ratio of momentum thickness to step height for thick boundary layer flow differed from those for thin boundary layer flow.

The present study was initiated to provide more information about an aft-facing discontinuity in thick boundary layer flow. The thick boundary layer flow results of this experiment are for different Reynolds number conditions than the previous studies and should provide more insight into the effect of Reynolds number on the drag levels associated with aft-facing discontinuities in a thick boundary layer. Because of its ability to maintain flight condition at speeds from subsonic to Mach 3, a YF-12 aircraft was selected as the facility for the experiment. Base pressure data were obtained for step heights of 0.33, 0.63, and 1.19 centimeters (0.13, 0.25, and 0.47 inch) at Mach numbers from 0.60 to approximately 3.00 with a range in altitude for many of the Mach numbers. The data presented here for the nominal Mach numbers of 2.20, 2.50, and 2.80 and a Reynolds number based on flow length of approximately 10^8 represent an analysis of an unclassified portion of the data set. These Mach numbers were selected to provide information that could be compared with results obtained by other experimenters. The momentum thickness for these data was approximately 0.25 centimeter (0.10 inch), and hence, the ratio of momentum thickness to step height ranged from 0.2 to nearly 1.0. Surface static pressures ahead of and behind the step were also measured and are presented as surface pressure distributions. A boundary layer rake was used to determine the velocity profiles and the local surface and boundary layer edge flow conditions.

SYMBOLS

Physical quantities in this report are given in the International System of Units (SI) and parenthetically in U.S. Customary Units. The measurements were taken in Customary Units. Factors relating the two systems are presented in reference 7.

a	constant, 1.0
b	constant, 20.5 (m/sec)/$K^{1/2}$ (49.02 (ft/sec)/(°R)$^{1/2}$)
c_F	average compressible skin friction coefficient
c_f	local compressible skin friction coefficient
c_{p_b}	base pressure coefficient, $\frac{p_b - p_r}{0.7M_\infty{}^2 p_r}$
d	diameter
h	step height ($2h$ is equivalent to trailing edge thickness of a wing)

K mixing length constant, 0.4

l length of flow from nose of aircraft to rake or step

M Mach number

p static pressure

R Reynolds number based on length l

R_θ Reynolds number based on momentum thickness

$S_{(\bullet)}$ standard deviation of subscripted variable

T static temperature, local value unless subscripted or superscripted

T' reference temperature (ref. 17)

T_t total or stagnation temperature

$$U = \frac{\left[(c_f/2)\sigma/(1-\sigma)\right]^{1/2}}{\arcsin\left(\sigma^{1/2}\right)}$$

u flow velocity

w width of rake strut

x longitudinal distance from step, distance forward of step is negative

y distance above aircraft surface (perpendicular to x)

γ ratio of specific heats for air, 1.4

δ boundary layer thickness

θ momentum thickness

μ absolute viscosity

Π coefficient of wake function

ρ air density

$$\sigma = \frac{[(\gamma-1)/2]M_e^2}{1+[(\gamma-1)/2]M_e^2}$$

φ	function dependent on Mach number and Reynolds number based on step height (ref. 20)
ψ	function dependent on Mach number and local compressible skin friction coefficient (ref. 20)

Superscript:

$'$	based on reference temperature

Subscripts:

b	step face, or base of aft-facing step
e	edge of boundary layer
r	local reference
∞	free stream

INSTRUMENTATION

The experiment reported in this paper was conducted on the upper surface of the fuselage of a YF-12 airplane. Figure 1 shows the airplane with the experiment installed. The fuselage diameter is 162.56 centimeters (64.00 inches).

The experiment required an aircraft surface contour change. The test section is shown in figure 2(a), and details are given in figure 2(b). The test section covered an area approximately 0.9 meter (2.9 feet) wide and 3.2 meters (10.5 feet) long and consisted of a ramp region, a reference region, a recovery region, and a boundary layer rake complex. The ramp region, which provided a gradual transition for the flow from the upper fuselage surface of the aircraft to the reference region, had a slope of approximately 1°7' relative to the surface of the aircraft. At the side edges, the three regions terminated in an abrupt step to the aircraft surface. The height of the recovery region could be changed between flights from a position level with the reference region to a position below the level of the reference region. Each position formed a right-angle step from the surface of the reference region to the surface of the recovery region, the maximum step height being 1.19 centimeters (0.47 inch). The step heights studied in this experiment were 0.33, 0.63, and 1.19 centimeters (0.13, 0.25, and 0.47 inch). The reference and recovery regions were parallel to within 0°40'. Pressure orifices were located along the surfaces of the reference and recovery regions and on the step face, as shown in figure 2(c). The locations of these orifices are given in table 1. The pressure measured at the orifice 20.42 centimeters (8.04 inches) ahead of the step was used as the local reference pressure. An average base pressure was determined by manifolding the pressures from the three base pressure orifices.

The boundary layer rake complex (fig. 3), which consisted of a boundary layer rake and a Preston probe, could be placed at one of two locations (fig. 2(a)): in

the reference region approximately 51 centimeters (20 inches) ahead of the step, or in the recovery region approximately 30 centimeters (12 inches) behind the step. The static pressure orifice for each boundary layer rake complex was in the skin surface directly ahead of the boundary layer rake. A static pressure probe was placed on the top rake probe for some of the flights of this study.

The boundary layer rake had 18 probes and consisted of a stainless steel strut with a 15° wedge-angle leading edge and a semicircular trailing edge. The leading edge of each of the probes on the rake was chamfered internally to a 30° included angle. The heights of the rake probes from the test section surface are given in table 2. Some design criteria for the boundary layer rake are shown in figure 4. The proportions of the rake were designed using criteria determined from wind tunnel evaluations of flight rakes tested in the NASA Ames Research Center's Unitary Plan Wind Tunnel. Parameters derived from these rakes in supersonic flow (ref. 8) were found to compare well with data from a single traversing probe.

The Preston probe used in this study was an impact pressure tube similar to that suggested by Preston (ref. 9) and calibrated in the study of reference 10. The leading edge of the cylindrical probe, or tube, was squared off perpendicular to the probe axis and was free of burrs. The probe had an outer diameter of 0.635 centimeter (0.250 inch), an inside-to-outside diameter ratio of 0.6, and a length of 6.35 centimeters (2.5 inches). Skin friction coefficients were derived using the calibration in reference 10.

The ramp, reference, and recovery regions were made of stainless steel. All joints resulting from the installation of the test apparatus that would affect the flow ahead of and behind the step were faired into the surrounding surface areas with a high temperature fairing compound. Some slots between the test section surface and the airplane surface were required along the sides and near the leading and trailing edges of the test installation for venting of trapped air and for heat expansion. All slots and gaps near the step were carefully sealed to insure that nearby venting did not affect the base pressure and that base bleed did not exist.

The pressure orifices in the surfaces of the reference and recovery regions were normal to the surface. The edges of the orifices were sharp (that is, free of observable radii) and free of burrs.

A 48-port multiplexing valve (Scanivalve) with a differential pressure transducer referenced to the local static reference pressure was used to measure the differential base pressure and the 34 static pressures ahead of and behind the step. The local static reference pressure was included in the pressure survey in front of the step; therefore, the Scanivalve transducer was referenced to itself for two ports and measured an in-flight zero with each complete cycle. The local static reference pressure, the base pressure, and the pressures at three orifices located 7.57, 25.35, and 30.43 centimeters (2.98, 9.98, and 11.98 inches) behind the step were also measured by individual differential pressure transducers. The differential transducers that measured the base pressures and the pressures at the orifices 7.57 and 25.35 centimeters (2.98 and 9.98 inches) behind the step were referenced to the local static reference pressure. The differential transducers that measured the pressures for the local static orifice and the orifice 30.43 centimeters (11.98 inches) behind the step were referenced to a plenum pressure obtained from a static orifice on the lower fuselage toward the front of the airplane. The plenum pressure was

measured by a high-resolution, absolute-pressure transducer which was kept in a carefully controlled temperature environment.

The 18 rake probe pressures were measured by two 48-port Scanivalves with differential transducers referenced to the plenum pressure, one Scanivalve transducer having a low range and the other a high range. Some of the rake probe pressures were measured on both Scanivalve transducers. The Preston probe pressure was measured on the low-range Scanivalve transducer and, for practically all the flights, was also measured with an individual differential pressure transducer referenced to the plenum pressure. The surface static pressure for the rake, the static probe pressure (measured by the static probe on the top probe of the rake), and the top probe impact rake pressure were measured on individual differential pressure transducers referenced to the plenum pressure. The range of the differential pressure transducer measuring the pressure from the top probe of the rake depended on whether or not the static probe was on the rake. All the ranges of the differential pressure transducers used in the experiment were chosen so that the pressures measured would vary throughout the range of the transducer.

Chromel-Alumel thermocouples were used to measure the local skin temperature. They were placed on the underside of the skin of the reference and recovery regions near the boundary layer complex. In addition, Chromel-Alumel thermocouples were used to monitor the temperature environment of the transducers, which assured that these instruments remained within acceptable temperature limits during flight.

Air data quantities were obtained from sensors on the aircraft's nose boom. The free-stream Mach number was obtained from onboard sensor data and was corrected with a calibration obtained from a combination of radar, radiosonde, and pacer aircraft data. The air data system is described in reference 11.

All the data obtained for the study were recorded on magnetic tape using a pulse code modulation (PCM) system. All records were synchronized by a time code generator.

ACCURACY

The Scanivalve transducer had a standard deviation of ± 158 N/m^2 (± 3.3 lb/ft^2). The standard deviation for the transducers measuring local reference static pressure and the static pressures for the rakes was ± 139 N/m^2 (± 2.9 lb/ft^2). The rake probe pressure transducers and Preston probe pressure transducer had standard deviations of ± 206 N/m^2 (± 4.3 lb/ft^2).

The standard deviations for the pressure ratios were found by using the following relationship, which was derived from equation (37) in reference 12:

$$S_{p/p_r} = \sqrt{\left[\frac{\partial (p/p_r)}{\partial p_r}\right]^2 \left(S_{p_r}\right)^2 + \left[\frac{\partial (p/p_r)}{\partial p}\right]^2 \left(S_p\right)^2}$$

This equation simplified to

$$S_{p/p_r} = \frac{1}{p_r}\sqrt{\left(-p/p_r\right)^2\left(S_{p_r}\right)^2 + \left(S_p\right)^2}$$

The standard deviations for p/p_r were ±0.015 for Mach 2.20, ±0.022 for Mach 2.50, and ±0.029 for Mach 2.80.

The data were obtained at stabilized flight conditions; therefore, pressure lag effects were negligible.

TEST CONFIGURATIONS AND CONDITIONS

Five configurations were tested. These configurations consisted of the following conditions: the boundary layer rake complex in the forward location; the boundary layer rake complex in the location behind the step for the no-step condition; and the boundary layer rake complex in the location behind the step for step heights of 0.33, 0.63, and 1.19 centimeters (0.13, 0.25, and 0.47 inch). Hereafter, these configurations will be referred to as the forward rake location, and the aft rake location with no step, the 0.33-centimeter (0.13-inch) step, the 0.63-centimeter (0.25-inch) step, or the 1.19-centimeter (0.47-inch) step. The aft locations are also referred to by the respective step heights alone. The forward and aft (no step) rake locations were used to determine reference boundary layer parameters for the step height data.

Data were obtained for a time period of 1 minute, beginning after the airplane had been established at steady-state flight conditions (that is, flight conditions for which the altitude and airspeed of the airplane were essentially constant). A 12-second time period was then chosen from the steadiest portion of each 1-minute time period, and the data from that period were analyzed. The same nominal Mach numbers of 2.20, 2.50, and 2.80 and their respective dynamic pressures were repeated for each configuration.

It was assumed that turbulent flow began at the nose of the airplane. The experiment was far enough downstream that the transition location did not affect the data. The length of turbulent flow from the airplane's nose to the leading edge of the boundary layer rake probes was 21.01 meters (68.94 feet) for the forward rake location and 21.86 meters (71.71 feet) for the aft rake location. The length of turbulent flow to the variable step was 21.53 meters (70.65 feet). The reference boundary layer parameters for the step location were considered to be an average of the parameters from the forward and aft rake locations.

RESULTS AND DISCUSSION

Boundary Layer Pressure Data

Data-reduction procedures. - Local Mach number values were determined from

the boundary layer impact pressures and the corresponding local static pressure by the method described in reference 13. The static pressure was assumed to be constant through the boundary layer. This assumption was supported by a comparison of the static pressure obtained from the rake tip static probe and the local surface static pressure. Local flow velocities were computed from local Mach number by assuming the total temperature to be constant through the boundary layer and equal to the free-stream value. The following expression was used:

$$u = bM\left(\frac{T_t}{1 + \frac{\gamma - 1}{2}M^2}\right)^{1/2}$$

Momentum thickness, θ, was calculated from the following flat-plate relationship:

$$\theta = \int_0^{\delta} \frac{\rho u}{\rho_e u_e}\left(1 - \frac{u}{u_e}\right)dy$$

Local skin friction coefficients were determined using the Preston, or surface impact, probe technique developed in reference 9. Compressibility effects were accounted for by using the calibration given in reference 10.

Data presentation. - In-flight velocity profiles were obtained for the five configurations of the experiment for each of the Mach numbers studied. The velocity profiles normalized to the velocity obtained from the probe most distant from the surface are shown in figures 5 and 6. Figure 5 compares the velocity profiles for the forward rake location with those for the aft rake location with no step; figure 6 shows the velocity profiles for the aft rake location with no step and with each of the three step heights. The velocity profiles for the aft rake location with the various step heights exhibit the same trend as the profile for the aft rake location with no step height, except for the pressure change caused by the expansion wave from the step.

In figure 5, the velocity ratio first appears to become constant with respect to distance above the surface at approximately 8 centimeters (3 inches) above the surface, thus indicating that the boundary layer has reached a uniform velocity. For distances greater than 13 centimeters (5 inches) above the surface, the velocity profile does not appear to be constant.

The reference boundary layer thickness parameters from the forward rake location and the aft (no step) rake location were calculated from the rake data for two outer edge conditions and are presented in table 3(a). One set of calculations assumed the edge conditions to be at the rake probe most distant from the surface, and the other set assumed the edge conditions to be at the rake probe approximately 13 centimeters (5 inches) from the surface. These sets of data are referred to herein as the full-rake profile and local profile data, respectively.

The full-rake profile data appear to be affected by flow from other parts of the aircraft, as evidenced by the velocity profile and by the significant but not consistent variations in momentum thickness values between the forward rake location and the aft (no step) rake location (table 3(a)). This variation in momentum thickness is also observed between the forward rake location data for a free-stream Mach number of 2.55 and those for Mach 2.57. The local profile does not have this

variation. Because of this and because the lower portion of these boundary layers is believed to dominate the step base pressure, the boundary layer parameters from the local profile were used to analyze the step base pressure data. Velocity profiles normalized to the velocity obtained from the probe approximately 13 centimeters (5 inches) from the surface are presented in figure 7 for the forward rake location and the aft (no step) rake location. (Note that the ordinate scale is expanded relative to that used in figures 5 and 6.)

Compressible, two-dimensional, turbulent momentum thickness values were predicted using the relationship $\theta = \frac{c_F x}{2}$, where c_F values were obtained using the information in references 14 and 15. The predicted momentum thickness values, presented in table 3(b), are larger than the measured values. A reason for this difference could be that the flow is not fully two-dimensional.

The two-dimensionality of the flow was further considered by comparing the measured velocity profiles for the local profile data with a predicted two-dimensional velocity profile (fig. 7). The relationship (ref. 16) used to predict the two-dimensional velocity profile,

$$\frac{u}{u_e} = \frac{1}{\sigma^{1/2}} \sin \left\{ \left(\arcsin \sigma^{1/2} \right) \left\{ 1 + \frac{1}{K} U \left[\ln (y/\delta) + \frac{2\left(1 - (y/\delta)^a\right)^{1/2}}{a} - \frac{2}{a} \ln \left[1 + \left(1 - (y/\delta)^a\right)^{1/2} \right] \right] - \frac{\Pi}{K} U (1 + \cos \pi y/\delta) \right\} \right\}$$

is for a compressible, turbulent, isoenergetic flow. Additional assumptions are that the boundary layer thickness, δ, is 13 centimeters (5 inches); K, the mixing length constant, is 0.4; a is 1.0, which is equivalent to assuming a linear shear stress distribution through the boundary layer; and Π is 0.55, which corresponds to $dp/dx = 0$. The predicted velocity profiles all have larger velocity defects than the measured velocity profile. This is consistent with the predicted momentum thickness values' being larger than the measured momentum thickness values. The velocity profile differences (and, hence, the differences in momentum thickness values) result from the upstream flow history and possibly from some three-dimensional effects; therefore, the flow is considered to be quasi-two-dimensional.

The local incompressible skin friction coefficient for the forward rake location and the aft (no step) rake location is presented in figure 8 as a function of Reynolds number based on momentum thickness. The data for the forward rake location and for the aft (no step) rake location are approximately 23 and 17 percent higher, respectively, than the von Kármán-Schoenherr flat-plate curve (ref. 14). This difference is consistent with the measured velocity profile's having a lesser velocity defect than expected. The data for incompressible conditions were obtained from the compressible data by using the reference temperature method described in reference 17. Local compressible skin friction coefficients for these rake locations are given in table 3(a). The skin friction coefficients used to analyze the base pressure data are an average of the skin friction coefficients for the forward rake location and the aft (no step) rake location (table 4).

Surface Pressure Data

The surface static pressures ahead of and behind the step were measured for each of the step heights and the no-step configuration. These data, although not analyzed in this report, are useful in confirming the zero pressure gradient assumption and are included for future reference and analysis. The ratio of these pressures with respect to the local reference pressure is shown as a function of distance from the step in figures 9, 10, and 11 for nominal Mach numbers of 2.20, 2.50, and 2.80, respectively. The pressure distributions for the various step heights have similar shapes. Figure 12 shows that the pressure rise occurs at the same normalized position, independent of Mach number, when distance from the step is expressed in terms of step height.

Base Pressure Data

The base pressure ratio, p_b/p_r, for a given Mach number is considered to be a function of the ratio of momentum thickness to step height, θ/h, with p_b/p_r increasing (drag decreasing) as θ/h increases. A considerable amount of base pressure data has been accumulated for θ/h values less than 0.1, as shown in references 18 and 19; however, base pressure data for θ/h values greater than 0.1 are limited. At least two flight experiments (the present study and that of ref. 6) and two wind tunnel experiments (refs. 4 and 5) have obtained base pressure data for θ/h values near 1.0. The base pressure data used in this study are summarized in table 4. Figure 13 shows the base pressure ratio for these four experiments as a function of θ/h for Mach numbers near 2.20, 2.50, and 2.80. All the data have the same trend of increasing base pressure ratio (decreasing drag) with increasing θ/h. However, the base pressure ratios from the various experiments are not always in good agreement, especially for values of θ/h near 1.0. The difference in the base pressure ratio for θ/h near 1.0 increases with Mach number from a base pressure ratio difference of less than 0.1 for Mach numbers near 2.20 to a difference of 0.2 for Mach numbers near 2.80. This suggests that for a given Mach number, p_b/p_r is a function of some other factor in addition to θ/h, such as Reynolds number based on momentum thickness, R_θ. Even though the data from the four experiments are compared for similar Mach numbers and θ/h values, the R_θ values vary, as shown in the keys in figure 13. The data appear to form a family of curves dependent on R_θ, the trend being lower values of p_b/p_r (increased drag) for a given θ/h as R_θ increases. The variation of base pressure ratio with R_θ is shown in figure 14. The effect of R_θ on base pressure ratio appears to be largest at the lower R_θ values.

A method of predicting the base pressure coefficient for surface discontinuities in turbulent flow (ref. 20) was derived from experimental data for surface discontinuities at an angle of attack of 0° and for zero heat transfer. The experimental drag values were obtained using a floating-element drag balance. The drag coefficients represent the loads on the discontinuity plus any changes in skin friction on the balance plate due to the discontinuity, less the skin friction on any part of the plate covered by the discontinuity. The method is considered to be applicable for surface discontinuities with heights up to one-tenth of the boundary layer thickness.

The predicted base pressure coefficient is calculated using the equation $c_{p_b} = (\psi - \varphi)c_f$, where φ is a function of Mach number and Reynolds number based on discontinuity height, and ψ is a function of Mach number and c_f. Values for ψ and φ are found by using the empirically determined curves of reference 20. Predicted base pressure coefficients were calculated using this method for the flow conditions of references 4 and 6 and the present study. The predicted base pressure coefficients for the flight data of the present study and of reference 6 were calculated using two sets of values for c_f and Reynolds number per unit length, R/l. One set used the experimentally determined values for c_f and R/l, and the other set used the aircraft's altitude and assumed standard atmosphere conditions to obtain a value for R/l. This predicted R/l was used to obtain a flat-plate-predicted value for c_f. The predicted base pressure coefficient for the wind tunnel data of reference 4 was calculated using an experimentally determined value for R/l and a predicted flat-plate value for c_f. The percentage differences between the measured base pressure coefficients and those predicted using the procedure in reference 20 are summarized in the following table.

Source of measured c_{p_b}	Source of predicted c_{p_b}	M	$\left(\frac{\text{Predicted } c_{p_b} - \text{Measured } c_{p_b}}{\text{Measured } c_{p_b}}\right)100$, percent	
			Average	Range
Wind tunnel (ref. 4)	Experimentally determined R/l; flat-plate-predicted c_f	2.41	25	13 to 40
Flight, present study	Experimentally determined R/l and c_f	2.20 2.50 2.80	25 24 30	20 to 32 22 to 27 28 to 31
	Predicted R/l; flat-plate-predicted c_f	2.20 2.50 2.80	-23 -24 -29	-20 to -27 -23 to -26 -28 to -30
Flight, XB-70 study (ref. 6)	Experimentally determined R/l and c_f	2.40	3	-4 to 11
	Predicted R/l; flat-plate-predicted c_f	2.40	2	-5 to 13

The XB-70 flight data (ref. 6) were obtained from an installation on the upper wing surface, and the flow field closely approximated flat-plate boundary layer flow conditions at an equivalent Mach number and Reynolds number. These flow conditions are known from a comparison of flight measurements and flat-plate predictions for the wing chordwise pressure distribution, local skin friction, and the boundary layer profile (ref. 21). Therefore, it is not surprising that the predictions, which were derived from flat-plate experiments, are in reasonably good agreement with the XB-70 flight data.

As previously discussed, the flow field for the present experiment was considered to be quasi-two-dimensional. The momentum thickness and skin friction

values differed from those that would have been predicted for flat-plate turbulent flow at an equivalent Mach number and Reynolds number. Therefore, it is not surprising that the prediction of the base pressure coefficient from the method of reference 20 is not in good agreement with the measured base pressure coefficient of the present study. As shown in the table, the predicted values when using a predicted R/l and flat-plate-predicted values of c_f are lower than the measured values. When measured values of c_f and R/l are used, the prediction error is of approximately the same magnitude but in the opposite direction.

The prediction based on Hastings' wind tunnel data (ref. 4) is not in good agreement with the wind tunnel data, even though the data were supposedly obtained for two-dimensional flow. It is not known why the disagreement is so great in this case.

CONCLUSIONS

High Reynolds number, turbulent flow data from an aft-facing step experiment were obtained from several flights of the YF-12 airplane for nominal Mach numbers of 2.20, 2.50, and 2.80. The data were analyzed and the base pressure data were compared with other flight and wind tunnel data and with a semiempirical estimate. The analysis led to the following conclusions:

1. The base pressure ratio data of the present study showed the same trend of increasing base pressure ratio (decreasing drag) with increasing ratio of momentum thickness to step height as previous experiments; however, the values of the base pressure ratios differed. The differences varied from less than 0.1 at Mach numbers near 2.20 to 0.2 at Mach numbers near 2.80 for ratios of momentum thickness to step height near 1.0. The differences were found to be a function of Reynolds number based on momentum thickness with the largest differences occurring at the lower values.

2. Surface static pressure rise occurred at the same normalized position, independent of Mach number, when distance from the step was expressed in terms of step height.

3. Measured base pressure coefficients were compared with base pressure coefficients calculated using a prediction method based on discontinuity data obtained in flat-plate boundary layer flow. The measured and predicted base pressure coefficients were in reasonably good agreement for flight data that had boundary layer thickness parameters and skin friction values close to those predicted for flat-plate turbulent flow at an equivalent Reynolds number. Two-dimensional wind tunnel data, however, did not agree well with the results of this prediction method. The data of the present study, which did not have values of skin friction and momentum thickness close to those predicted for flat-plate turbulent flow at an equivalent Reynolds number, did not agree with base pressure coefficients from the prediction methods.

NASA Dryden Flight Research Center
Edwards, Calif., June 22, 1977

REFERENCES

1. Korst, H. H.: A Theory for Base Pressures in Transonic and Supersonic Flow. J. Appl. Mech., vol. 23, no. 4, Dec. 1956, pp. 593-600.

2. Chapman, Dean R.: An Analysis of Base Pressure at Supersonic Velocities and Comparison With Experiment. NACA Rept. 1051, 1951. (Supersedes NACA TN 2137.)

3. Chapman, Dean R.; Wimbrow, William R.; and Kester, Robert H.: Experimental Investigation of Base Pressure on Blunt-Trailing-Edge Wings at Supersonic Velocities. NACA Rept. 1109, 1952. (Supersedes NACA TN 2611.)

4. Hastings, R. C.: Turbulent Flow Past Two-Dimensional Bases in Supersonic Streams. R. & M. No. 3401, British A.R.C., 1965.

5. Moore, D. R.: Drag Effects of Surface Roughness at High Reynolds Numbers, M = 2.8. Report No. 0-71000/4R-16, LTV Research Center, 1964.

6. Goecke, Sheryll A.: Flight-Measured Base Pressure Coefficients for Thick Boundary-Layer Flow Over an Aft-Facing Step for Mach Numbers From 0.4 to 2.5. NASA TN D-7202, 1973.

7. Mechtly, E. A.: The International System of Units - Physical Constants and Conversion Factors. Second Revision. NASA SP-7012, 1973.

8. Keener, Earl R.; and Hopkins, Edward J.: Accuracy of Pitot-Pressure Rakes for Turbulent Boundary-Layer Measurements in Supersonic Flow. NASA TN D-6229, 1971.

9. Preston, J. H.: The Determination of Turbulent Skin Friction by Means of Pitot Tubes. No. 15,758, British A.R.C., Mar. 31, 1953.

10. Hopkins, Edward J.; and Keener, Earl R.: Study of Surface Pitots for Measuring Turbulent Skin Friction at Supersonic Mach Numbers—Adiabatic Wall. NASA TN D-3478, 1966.

11. Larson, Terry J.: Compensated and Uncompensated Nose Boom Static Pressures Measured From Two Air Data Systems on a Supersonic Airplane. NASA TM X-3132, 1974.

12. Beers, Yardley: Introduction to the Theory of Error. Second ed., Addison-Wesley Publishing Co., Inc., 1962.

13. Ames Research Staff: Equations, Tables, and Charts for Compressible Flow. NACA Rept. 1135, 1953. (Supersedes NACA TN 1428.)

14. Locke, F. W. S., Jr.: Recommended Definition of Turbulent Friction in Incompressible Fluids. DR Rept. No. 1415, Navy Dept., Bur. of Aeronautics, Res. Div., June 1952.

15. Bertram, Mitchel H.: Calculations of Compressible Average Turbulent Skin Friction. NASA TR R-123, 1962.

16. Sun, Chen-Chih; and Childs, Morris E.: A Modified Wall Wake Velocity Profile for Turbulent Compressible Boundary Layers. J. Aircraft, vol. 10, no. 6, June 1973, pp. 381-383.

17. Sommer, Simon C.; and Short, Barbara J.: Free-Flight Measurements of Turbulent-Boundary-Layer Skin Friction in the Presence of Severe Aerodynamic Heating at Mach Numbers From 2.8 to 7.0. NACA TN 3391, 1955.

18. McDonald, H.: The Turbulent Supersonic Base Pressure Problems - a Comparison between a Theory and some Experimental Evidence. Rept. No. Ae 194, British Aircraft Corporation, Preston Div., Apr. 1965.

19. Nash, J. F.: An Analysis of Two-Dimensional Turbulent Base Flow, Including the Effect of the Approaching Boundary Layer. NPL Aero Rep. 1036, British A.R.C., July 30, 1962.

20. Drag of two-dimensional steps and ridges immersed in a turbulent boundary layer at subsonic and supersonic speeds. Item Number 73028, Engineering Sciences Data Unit, Oct. 1973.

21. Fisher, David F.; and Saltzman, Edwin J.: Local Skin Friction Coefficients and Boundary-Layer Profiles Obtained in Flight From the XB-70-1 Airplane at Mach Numbers Up to 2.5. NASA TN D-7220, 1973.

TABLE 1.—SURFACE PRESSURE ORIFICE LOCATIONS

(a) Reference and recovery regions

Longitudinal position with respect to step	Distance from and lateral position with respect to experiment centerline, cm (in.)				
	2.54 (1.00) left	1.27 (0.50) left	0 (0)	1.27 (0.50) right	2.54 (1.00) right
	x, cm (in.)				
Forward	---	---	-54.25 (21.36)	---	---
	---	---	-25.50 (10.04)[a]	---	---
	---	---	-20.42 (8.04)[b]	---	---
	---	---	-15.34 (6.04)	---	---
	---	---	-10.26 (4.04)	---	---
	---	---	-5.05 (1.99)	---	---
	---	-3.78 (1.49)	---	---	---
	---	---	-1.88 (0.74)	---	---
	---	---	---	-1.30 (0.51)	---
	---	---	-0.66 (0.26)	---	---
Aft	---	---	0.58 (0.23)	---	---
	---	---	---	---	1.24 (0.49)
	---	---	---	1.85 (0.73)	---
	---	---	2.49 (0.98)	---	---
	---	3.12 (1.23)	---	---	---
	3.76 (1.48)	---	---	---	---
	---	---	---	4.39 (1.73)	---
	---	---	5.03 (1.98)	---	---
	---	5.66 (2.23)	---	---	---
	---	---	---	---	6.30 (2.48)
	---	---	---	6.93 (2.73)	---
	---	---	7.57 (2.98)	---	---
	---	8.20 (3.23)	---	---	---
	8.86 (3.49)	---	---	---	---
	---	---	---	9.47 (3.73)	---
	---	---	10.11 (3.98)	---	---
	---	11.38 (4.48)	---	---	---
	---	---	12.67 (4.99)	---	---
	---	---	---	13.92 (5.48)	---
	---	---	15.21 (5.99)	---	---
	---	16.48 (6.48)	---	---	---
	---	---	17.73 (6.98)	---	---
	---	---	20.27 (7.98)	---	---
	---	---	25.35 (9.98)	---	---
	---	---	30.43 (11.98)[c]	---	---

[a]Surface static pressure orifice for forward rake complex.

[b]Local reference pressure orifice.

[c]Surface static pressure orifice for aft rake complex.

TABLE 1.—Concluded

(b) Step face

h, cm (in.)	Position with respect to experiment centerline—		Depth from reference region, cm (in.)
	Left	Right	
	Distance from centerline, cm (in.)		
0.33 (0.13)	7.65 (3.01)	---	0.15 (0.06)
	1.30 (0.51)	---	0.15 (0.06)
	---	5.59 (2.20)	0.15 (0.06)
0.63 (0.25)	5.36 (2.11)	---	0.30 (0.12)
	1.30 (0.51)	---	0.15 (0.06)
	---	6.65 (2.62)	0.30 (0.12)
1.19 (0.47)	6.38 (2.51)	---	0.38 (0.15)
	1.30 (0.51)	---	0.89 (0.35)
	---	7.75 (3.05)	0.64 (0.25)

TABLE 2.—HEIGHTS OF BOUNDARY LAYER RAKE PROBES

Boundary layer rake position	
Forward[a]	Aft[b]
Distance from test section surface to centerline of probe, cm (in.)	
0.490 (0.193)	0.401 (0.158)
1.760 (0.693)	1.694 (0.667)
3.030 (1.193)	2.951 (1.162)
4.313 (1.698)	4.249 (1.673)
5.56 (2.19)	5.54 (2.18)
7.54 (2.97)	7.52 (2.96)
10.08 (3.97)	10.06 (3.96)
12.57 (4.95)	12.55 (4.94)
15.11 (5.95)	15.11 (5.95)
20.17 (7.94)	20.17 (7.94)
25.25 (9.94)	25.27 (9.95)
30.33 (11.94)	30.35 (11.95)
35.41 (13.94)	35.43 (13.95)
40.49 (15.94)	40.49 (15.94)
45.57 (17.94)	45.54 (17.93)
50.67 (19.95)	50.62 (19.93)
55.78 (21.96)	55.73 (21.94)
----	60.83 (23.95)

[a]Static probe was always attached when rake was in forward location.

[b]Probe heights for aft rake location represent average values for various step height configurations. The rake probe heights changed slightly with each step height configuration because the relative vertical position of the boundary layer rake could not be maintained exactly when the step height was changed. The measured rake probe heights for each configuration were used in the calculations for that configuration.

TABLE 3.—BOUNDARY LAYER THICKNESS PARAMETERS

(a) Measured parameters for reference conditions

Rake location	l (to rake), m (ft)	M_∞	c_f	Full-rake profile				Local profile			
				δ, cm (in.)	M_e	θ, cm (in.)	R_θ	δ, cm (in.)	M_e	θ, cm (in.)	R_θ
Forward	21.01 (68.94)	2.17	0.00210	55.78 (21.96)	2.26	0.86 (0.34)	4.46×10^4	12.57 (4.95)	2.16	0.28 (0.11)	1.28×10^4
		2.49	0.00204	55.78 (21.96)	2.57	0.84 (0.33)	3.86	12.57 (4.95)	2.42	0.25 (0.10)	0.96
		2.81	0.00200	55.78 (21.96)	2.86	0.56 (0.22)	2.26	12.57 (4.95)	2.72	0.23 (0.09)	0.83
Aft (no step)	21.86 (71.71)	2.27	0.00187	60.81 (23.94)	2.21	0.33 (0.13)	1.68	12.55 (4.94)	2.22	0.30 (0.12)	1.53
		2.55	0.00195	55.78 (21.96)	2.52	0.48 (0.19)	1.85	12.55 (4.94)	2.47	0.25 (0.10)	0.91
		2.57	0.00190	60.81 (23.94)	2.58	0.81 (0.32)	3.67	12.55 (4.94)	2.48	0.25 (0.10)	1.03
		2.85	0.00193	55.78 (21.96)	2.84	0.79 (0.31)	2.89	12.55 (4.94)	2.70	0.23 (0.09)	0.75

(b) Predicted parameters. l = 21.53 meters (70.65 feet) to step.

M	R	θ, $c_f x/2$, cm (in.)
2.20	1.05×10^8	1.63 (0.64)
2.50	0.90	1.47 (0.58)
2.80	0.77	1.37 (0.54)

TABLE 4.—MEASURED STEP PARAMETERS

[θ, R_θ, and c_f obtained at reference conditions]

h, cm (in.)	M_∞	p_b/p_r	θ, cm (in.)	R_θ	c_f
0.33 (0.13)	2.26	0.55	0.28 (0.11)	1.40×10^4	0.00198
0.63 (0.25)	2.23	0.48			
1.19 (0.47)	2.23	0.45			
0.33 (0.13)	2.54	0.50	0.25 (0.10)	0.96	0.00198
0.63 (0.25)	2.50	0.43			
1.19 (0.47)	2.50	0.38			
0.33 (0.13)	2.89	0.51	0.23 (0.09)	0.79	0.00196
0.63 (0.25)	2.85	0.42			
1.19 (0.47)	2.81	0.34			

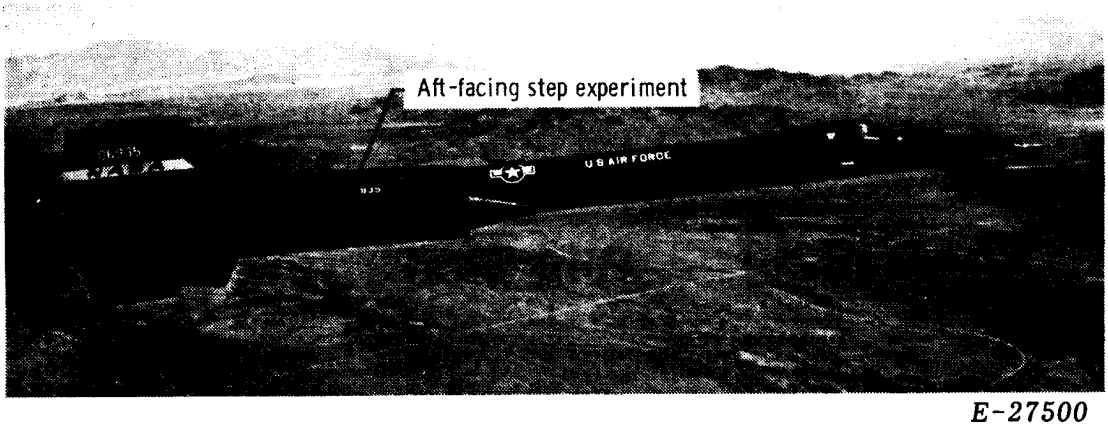

E-27500

Figure 1. YF-12 airplane in flight, showing location of aft-facing step experiment.

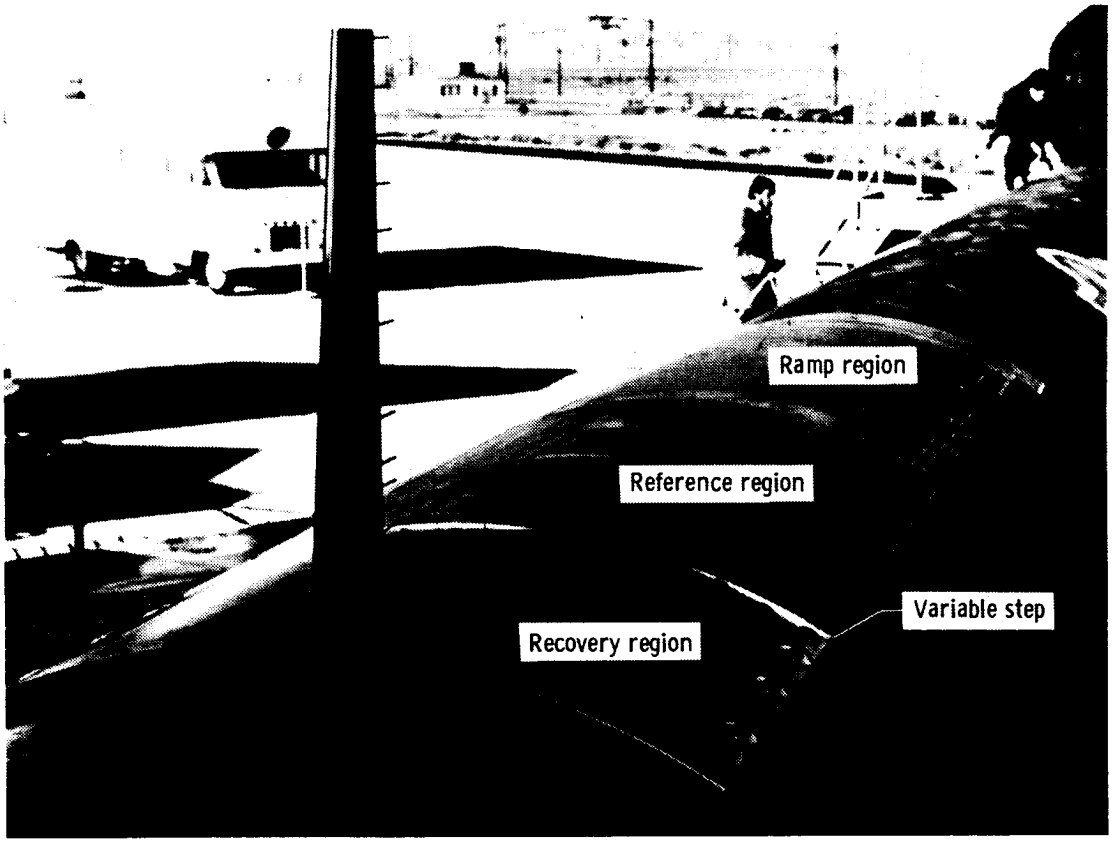

E-26695

(a) Test section viewed from rear. Boundary layer rake complex is in aft location; step height is 0.63 centimeters (0.25 inch).

Figure 2. Aft-facing step experiment test section with details of component and orifice locations.

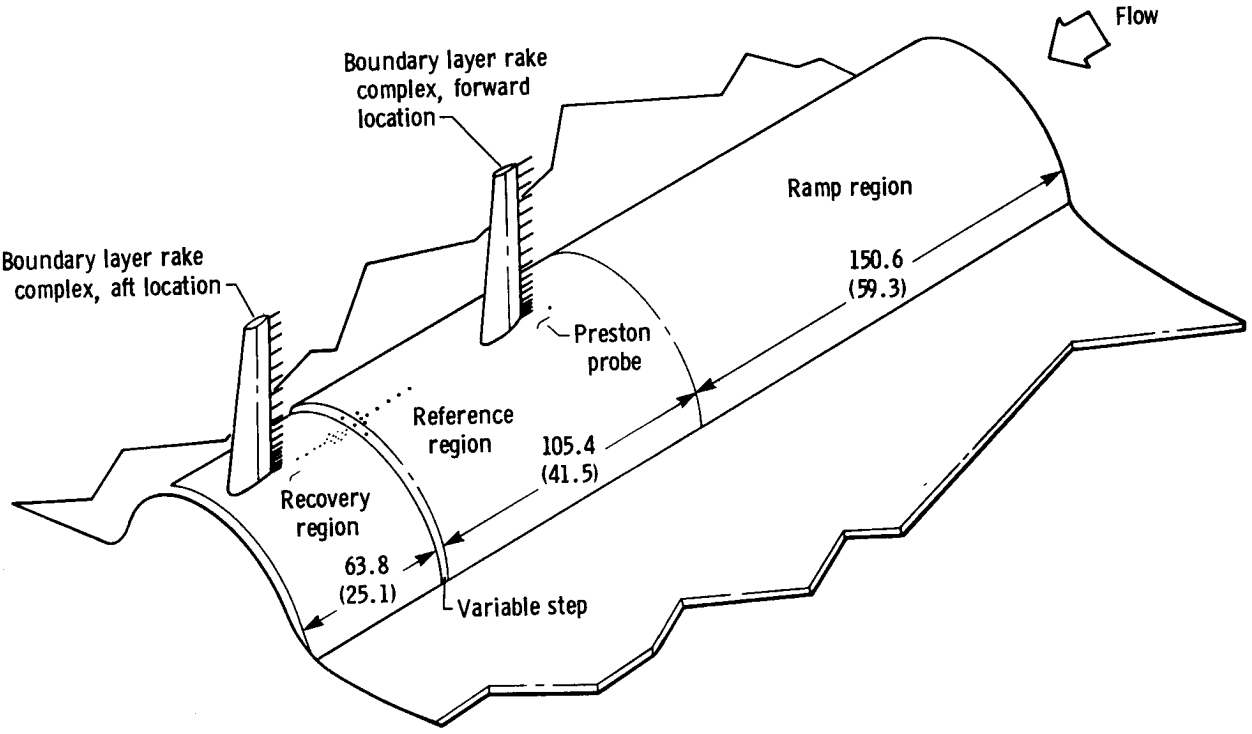

(b) Details of component locations. Dimensions are in centimeters (inches).

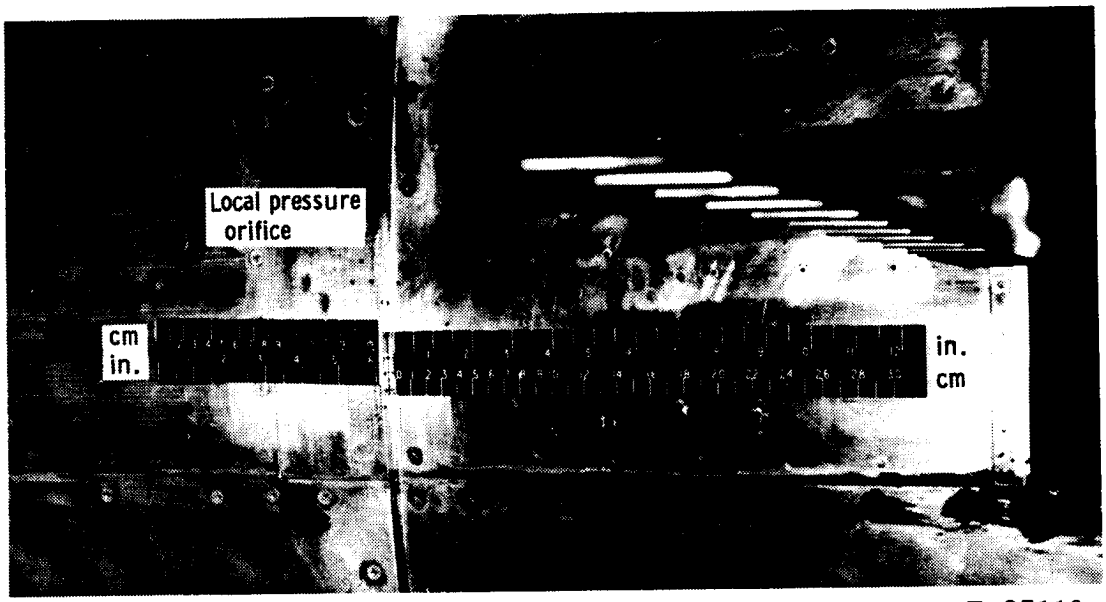

E-27110

(c) View of step region showing location of pressure orifices. Step height is 1.19 centimeters (0.47 inch).

Figure 2. Concluded.

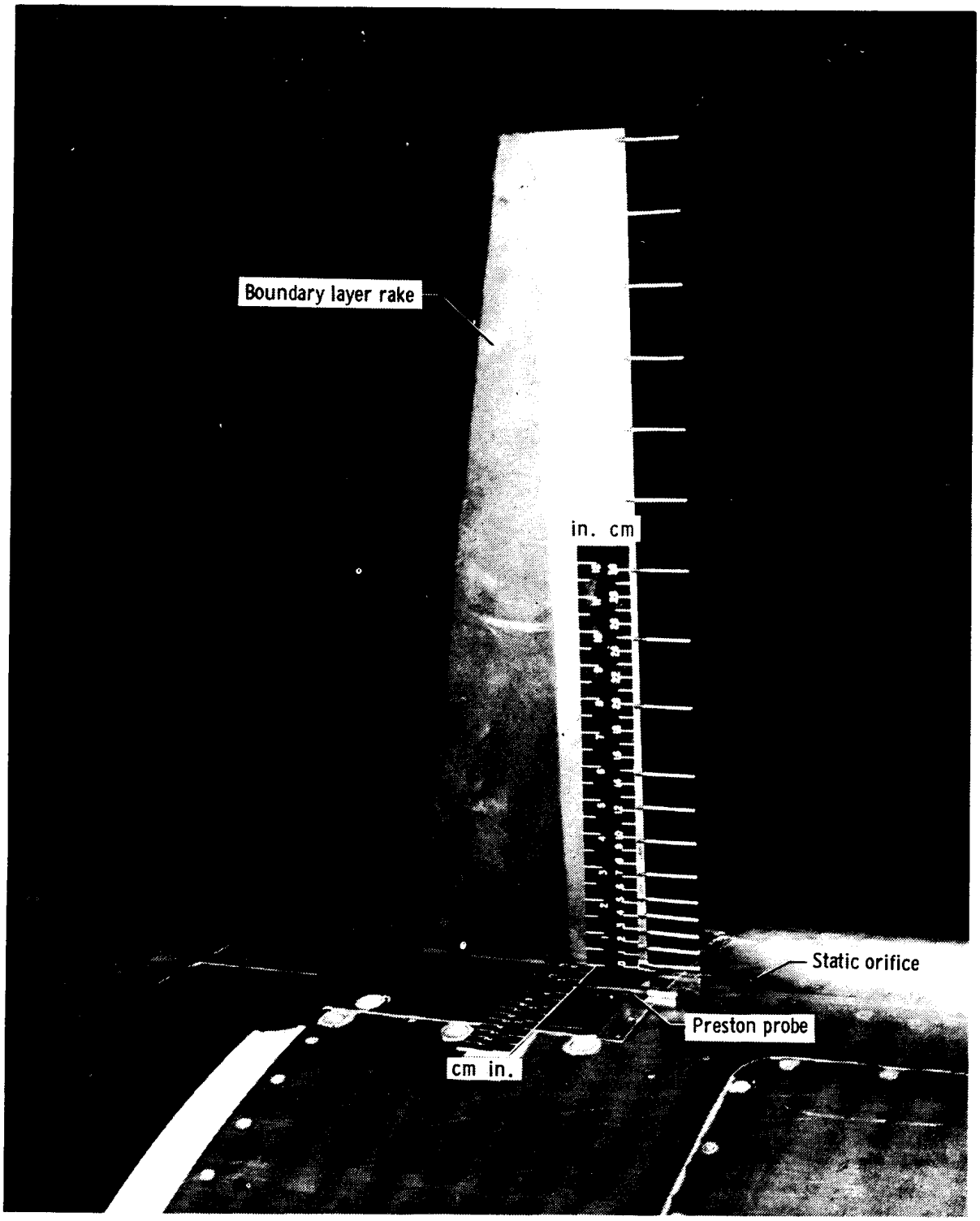

Figure 3. Boundary layer rake complex.

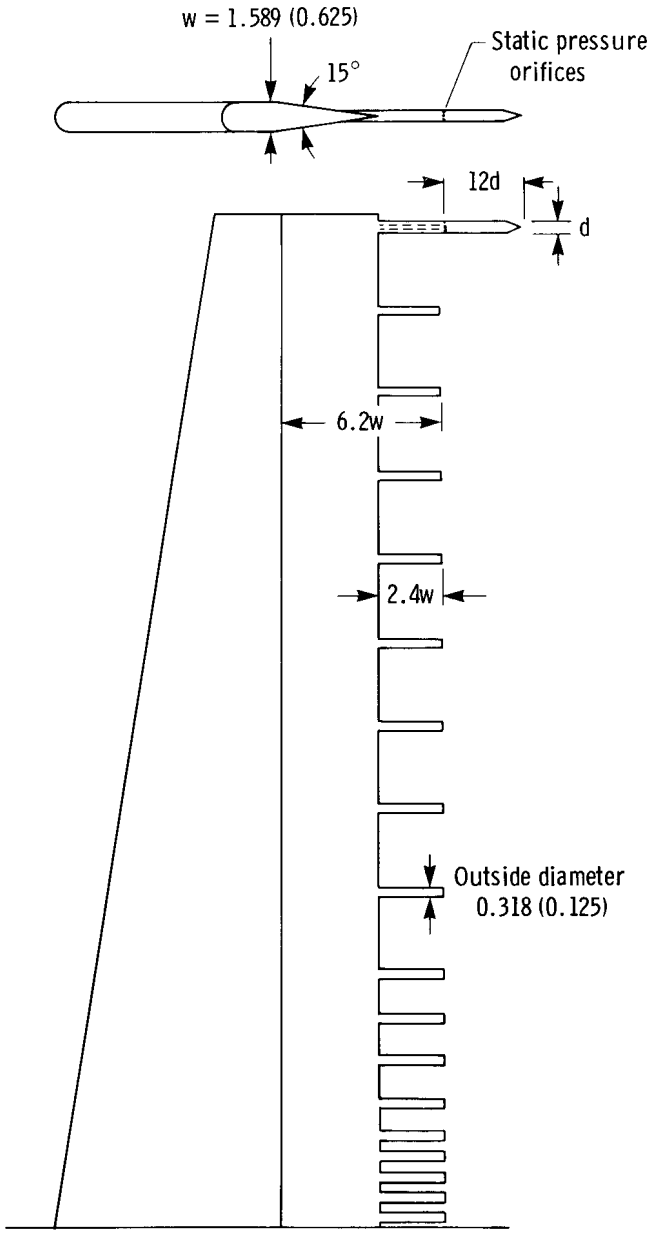

Figure 4. Two views of boundary layer rake showing some design criteria. Dimensions are in centimeters (inches).

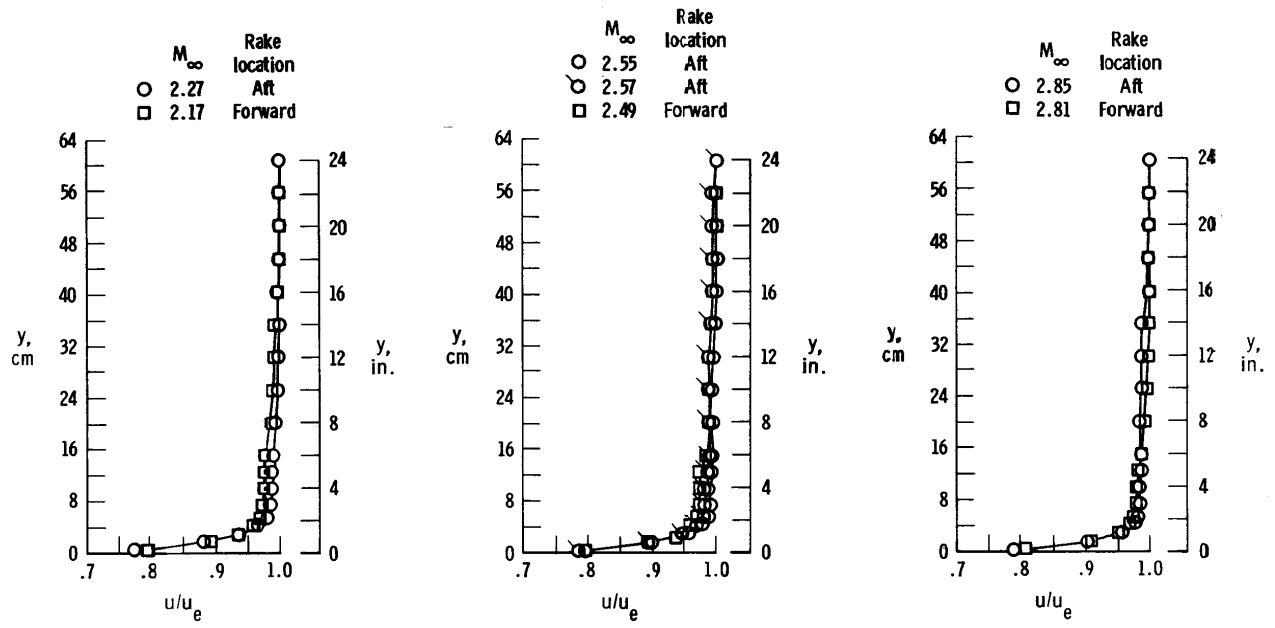

(a) $M_\infty \approx 2.20$.

(b) $M_\infty \approx 2.50$.

(c) $M_\infty \approx 2.80$.

Figure 5. Velocity profiles for forward and aft (no step) rake locations. u_e obtained from probe most distant from aircraft surface.

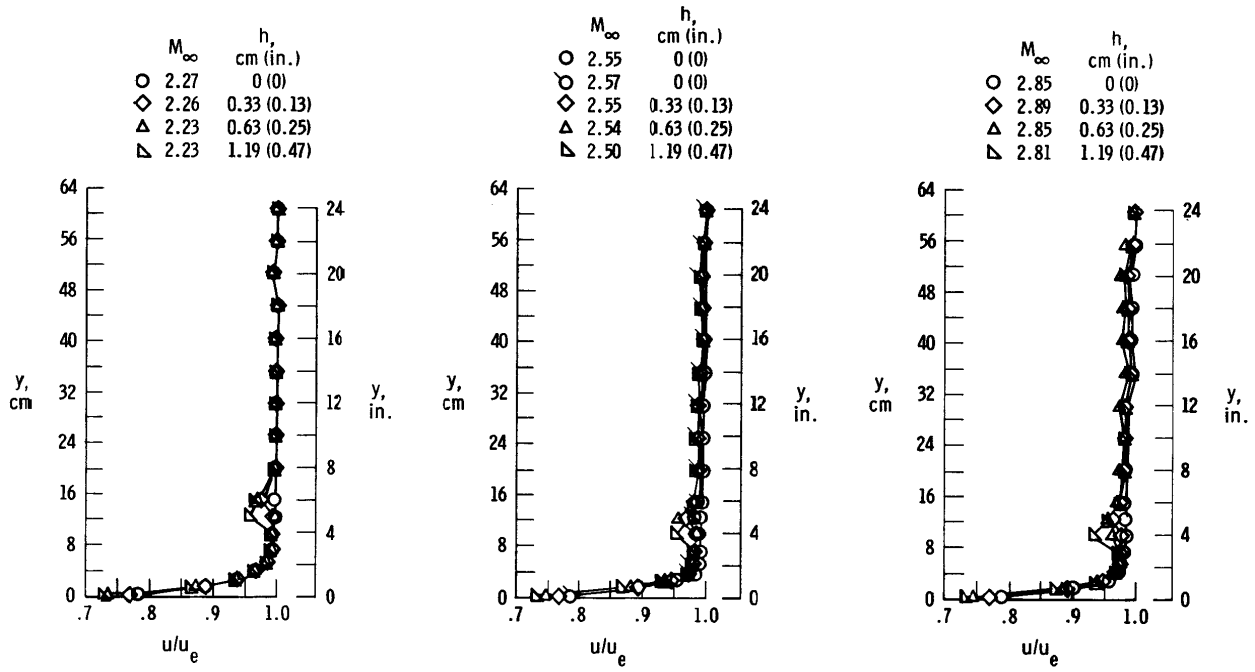

(a) $M_\infty \approx 2.20$.

(b) $M_\infty \approx 2.50$.

(c) $M_\infty \approx 2.80$.

Figure 6. Velocity profiles for aft rake location with various step heights. u_e obtained from probe most distant from aircraft surface.

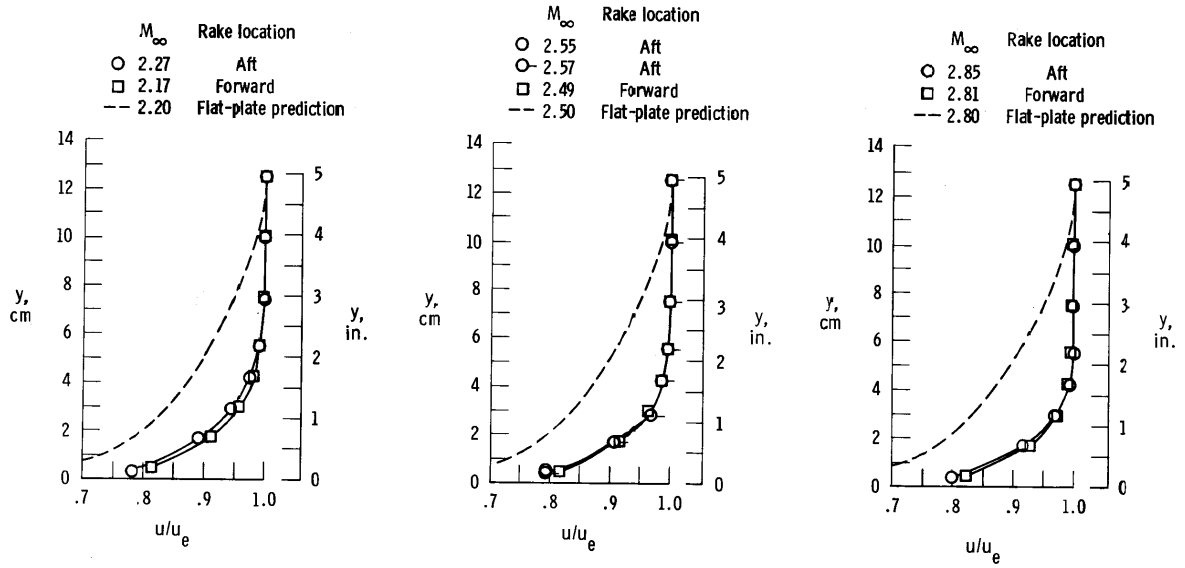

(a) $M_\infty \approx 2.20$.

(b) $M_\infty \approx 2.50$.

(c) $M_\infty \approx 2.80$.

Figure 7. Local velocity profiles for the forward and aft (no step) rake locations. u_e obtained from probe approximately 13 centimeters (5 inches) above surface; flat-plate prediction method is from reference 16.

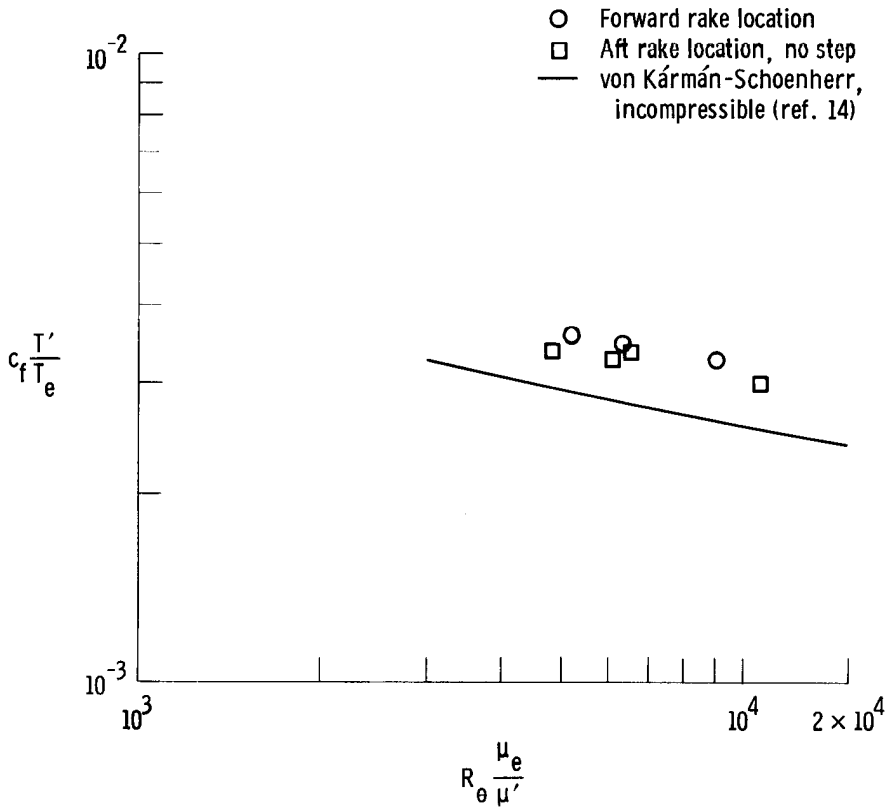

Figure 8. Variation of local skin friction coefficient with Reynolds number based on momentum thickness for forward and aft (no step) rake locations; data transformed to incompressible conditions.

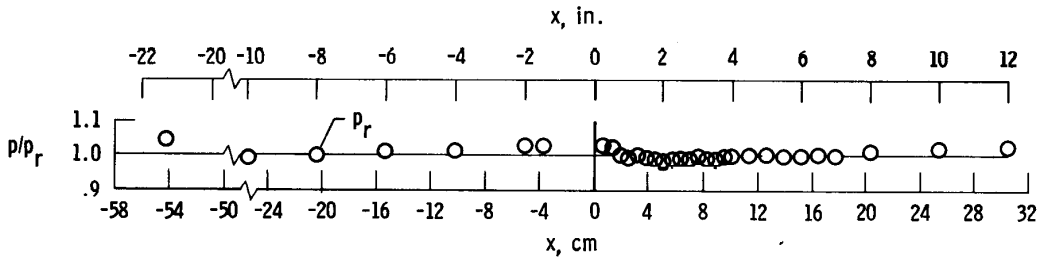

(a) No step; $M_e = 2.27$.

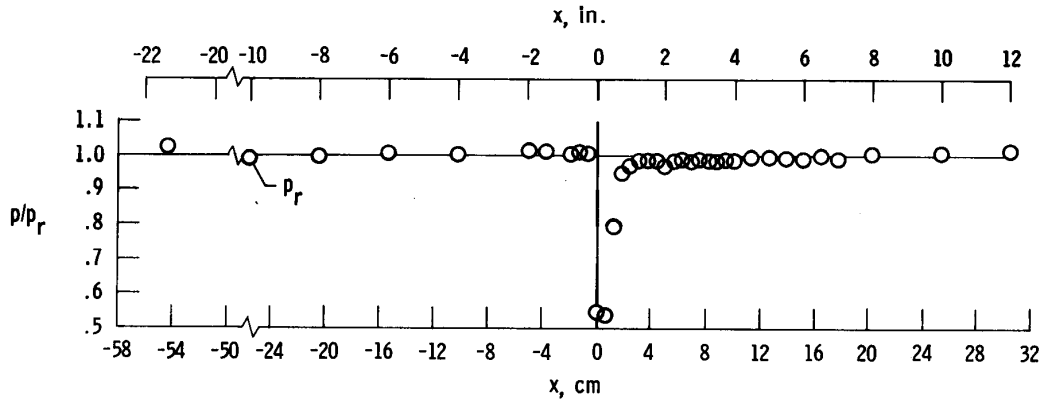

(b) h = 0.33 cm (0.13 in.); $M_e = 2.26$.

Figure 9. Variation of pressure ratio with distance from step for Mach numbers near 2.20.

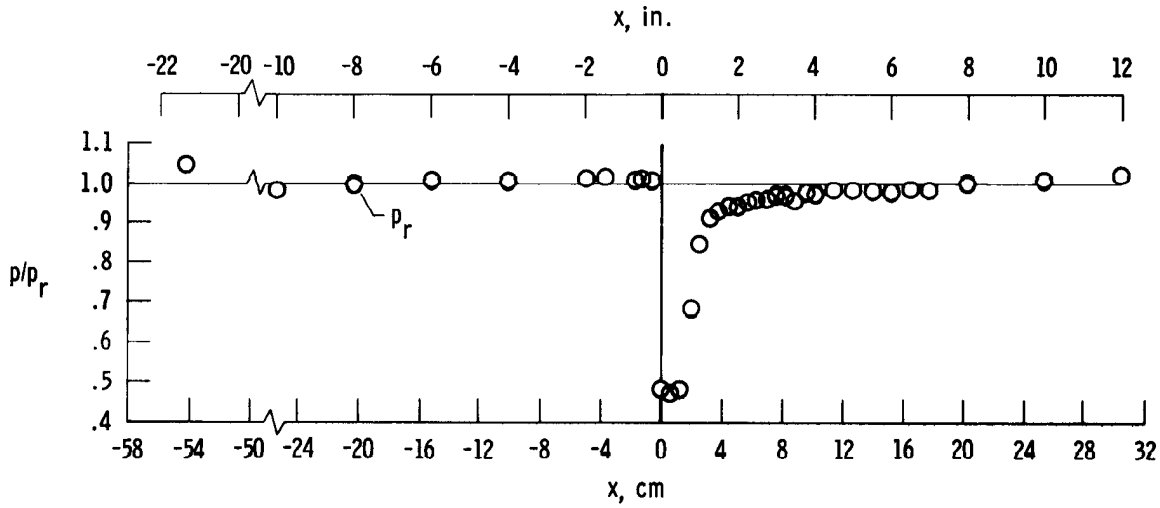

(c) h = 0.63 cm (0.25 in.); M_∞ = 2.23.

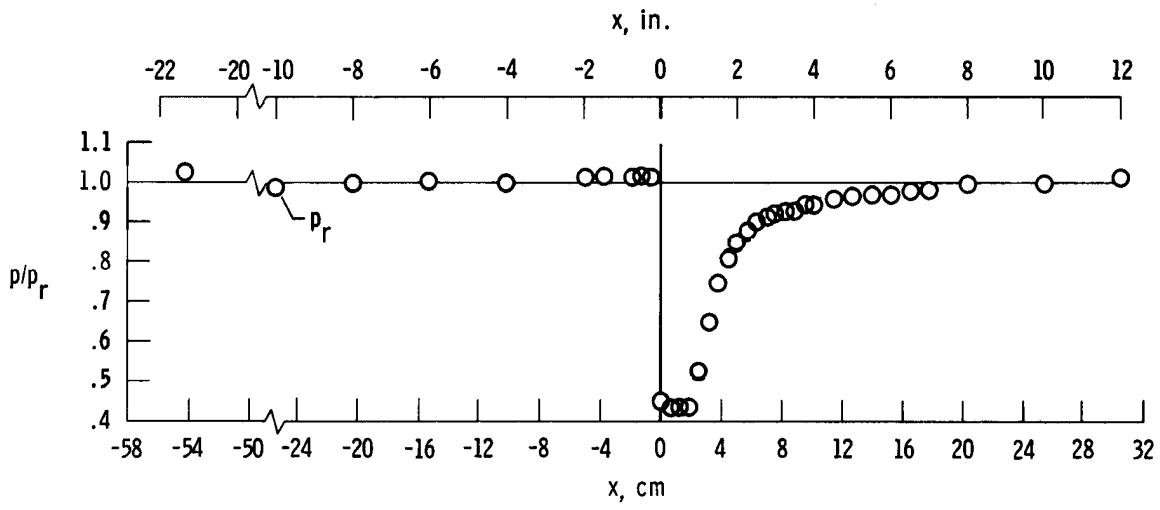

(d) h = 1.19 cm (0.47 in.); M_∞ = 2.23.

Figure 9. Concluded.

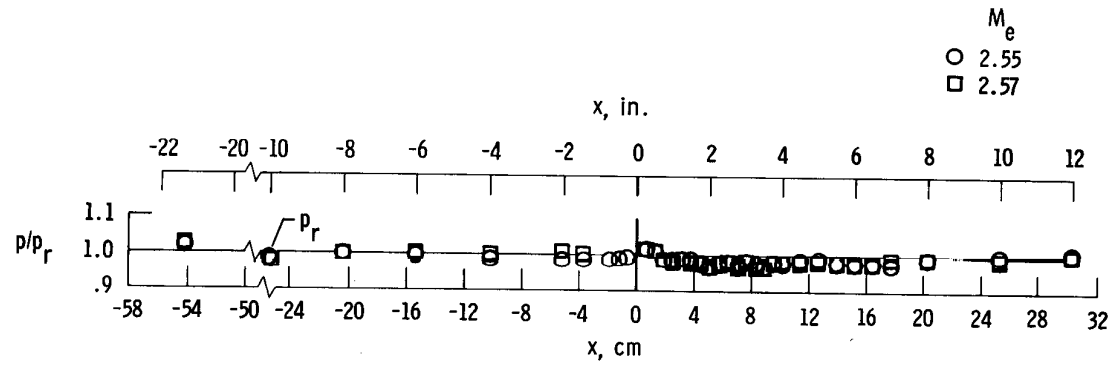

(a) No step.

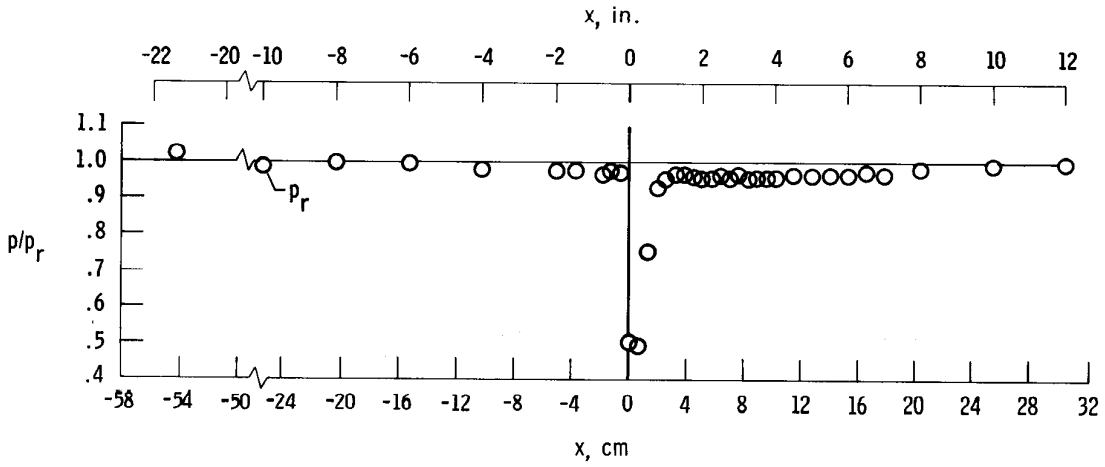

(b) $h = 0.33$ cm (0.13 in.); $M_e = 2.47$.

Figure 10. Variation of pressure ratio with distance from step for Mach numbers near 2.50.

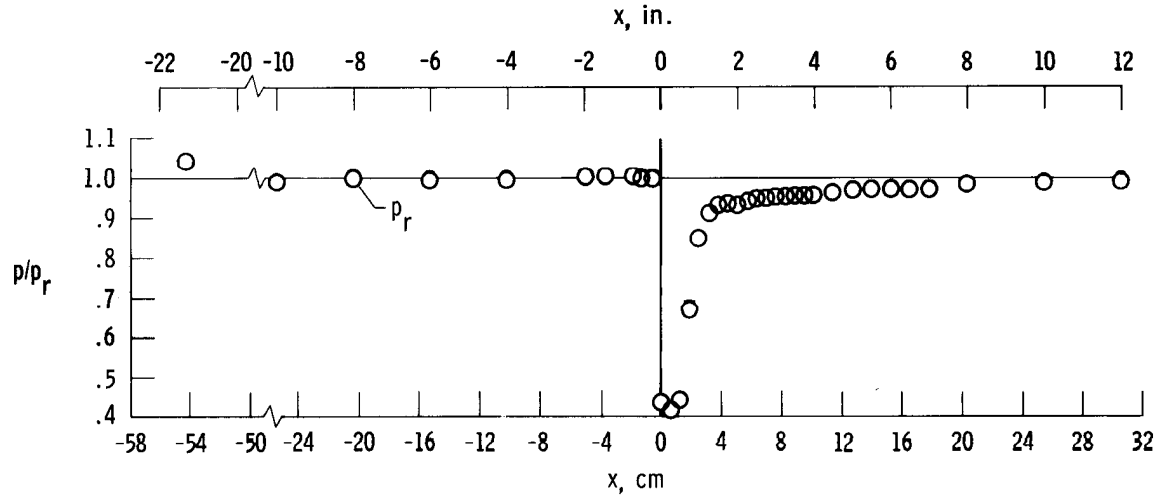

(c) h = 0.63 cm (0.25 in.); M_e = 2.50.

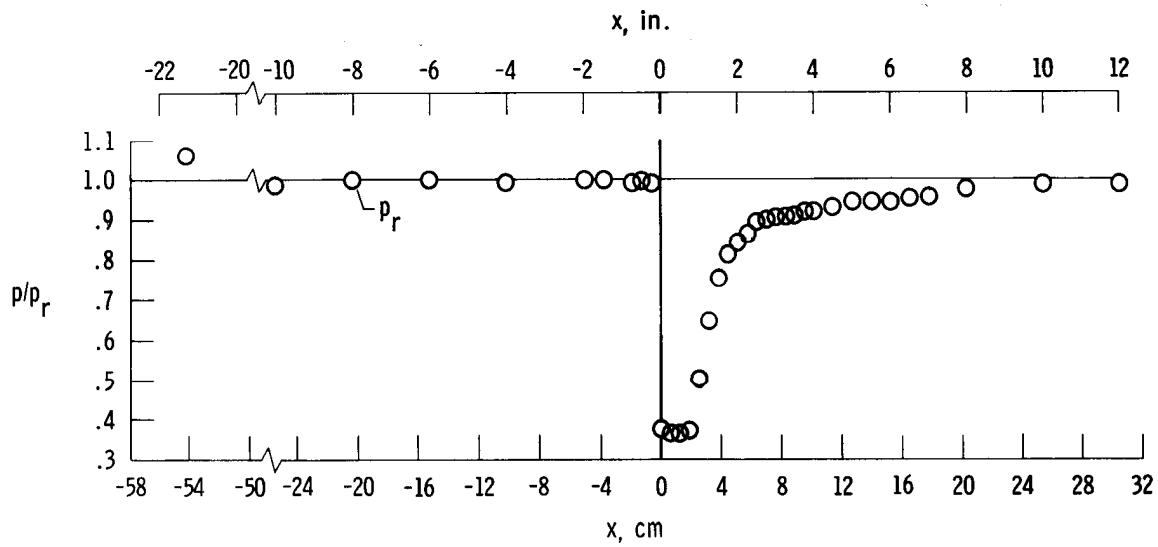

(d) h = 1.19 cm (0.47 in.); M_e = 2.50.

Figure 10. Concluded

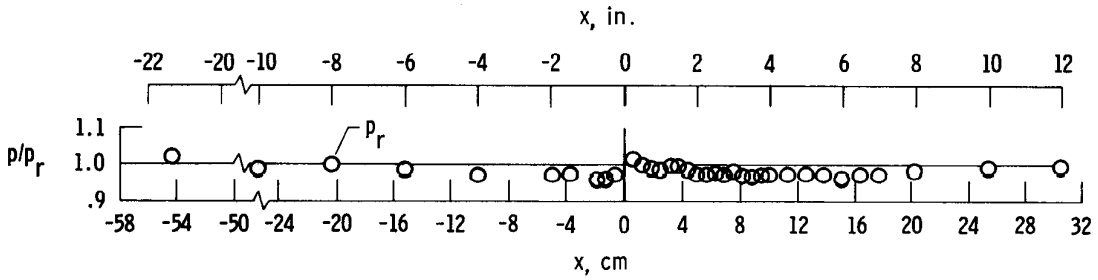

(a) No step; $M_e = 2.85$.

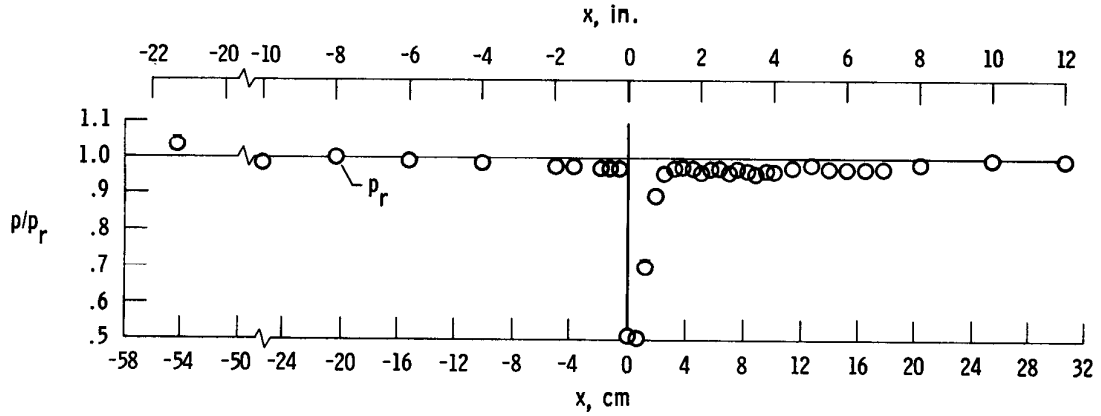

(b) $h = 0.33$ cm (0.13 in.); $M_e = 2.89$.

Figure 11. Variation of pressure ratio with distance from step for Mach numbers near 2.80.

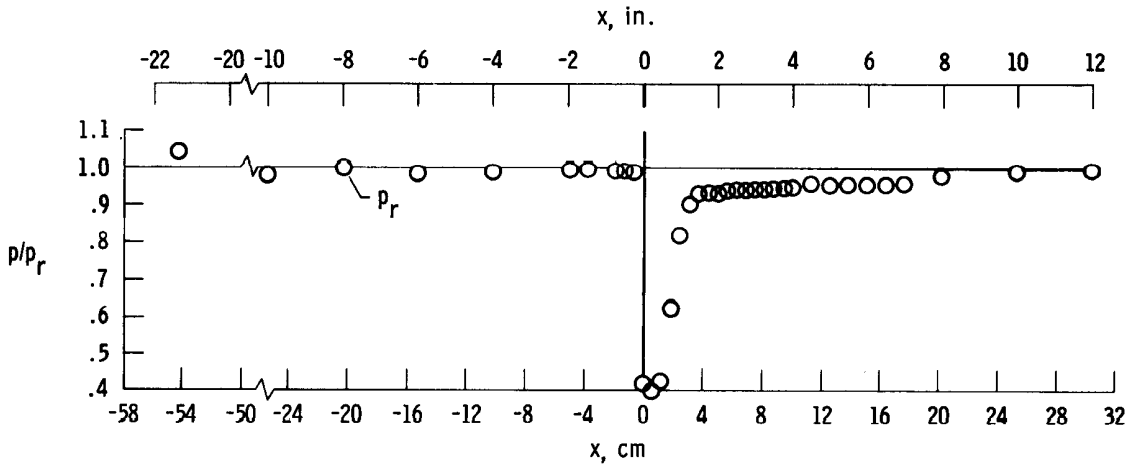

(c) h = 0.63 cm (0.25 in.); M_e = 2.85.

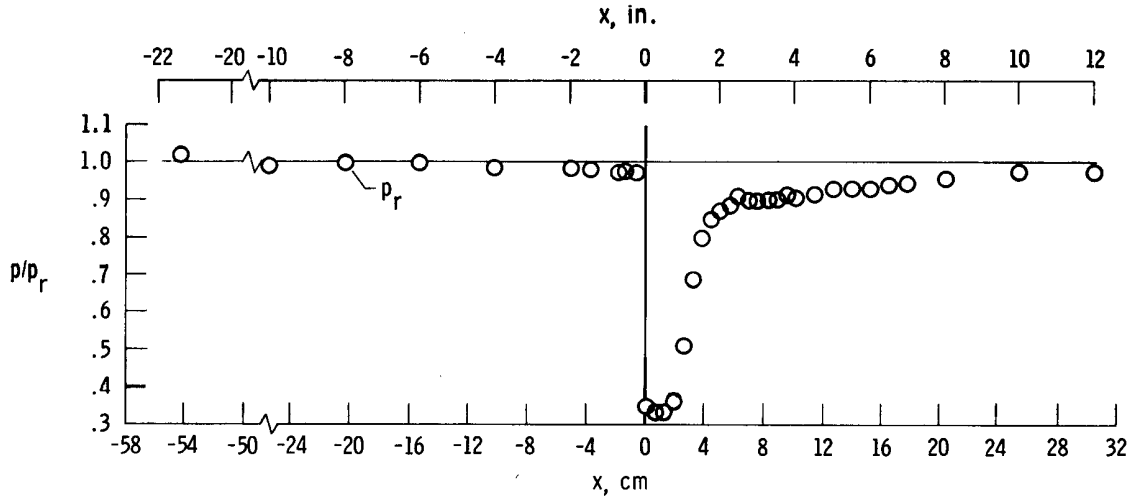

(d) h = 1.19 cm (0.47 in.); M_e = 2.81.

Figure 11. Concluded.

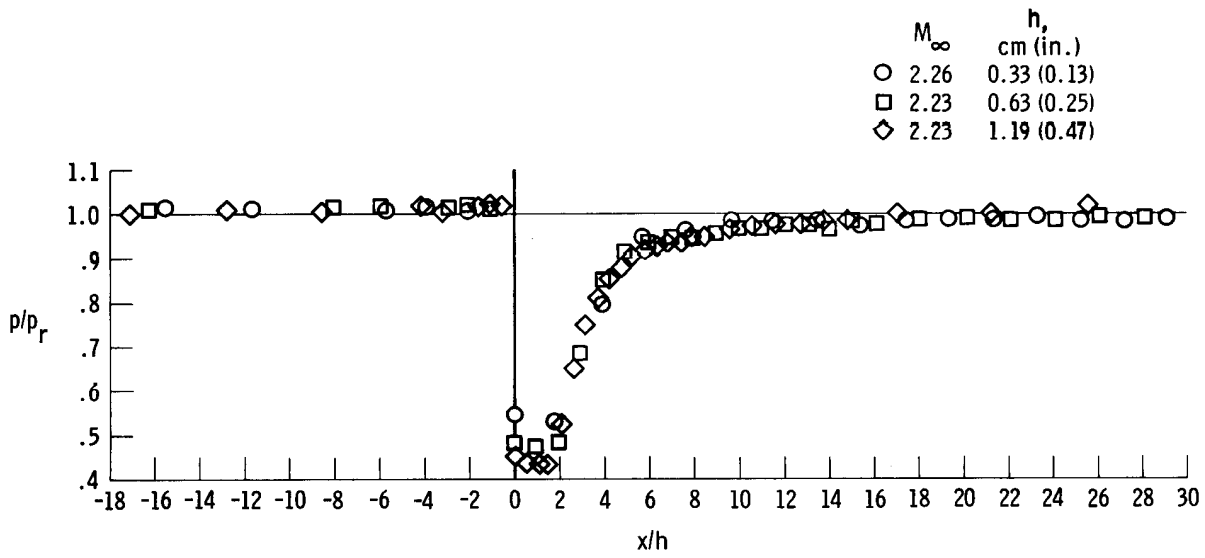

(a) $M_\infty \approx 2.20$.

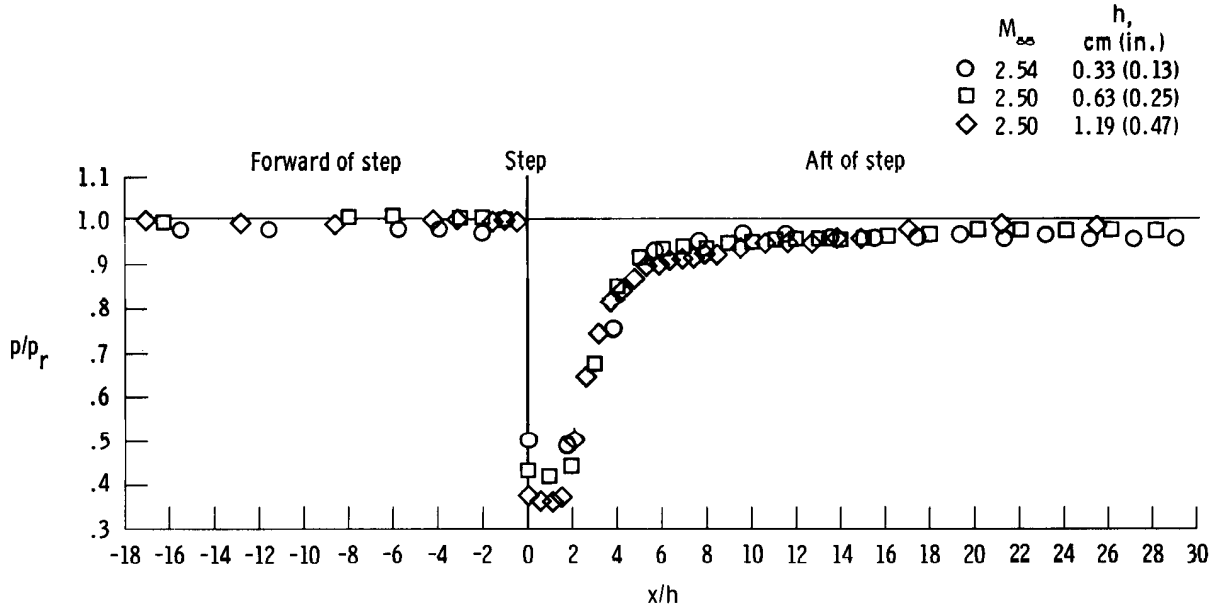

(b) $M_\infty \approx 2.50$.

Figure 12. Variation of pressure ratio as function of step height.

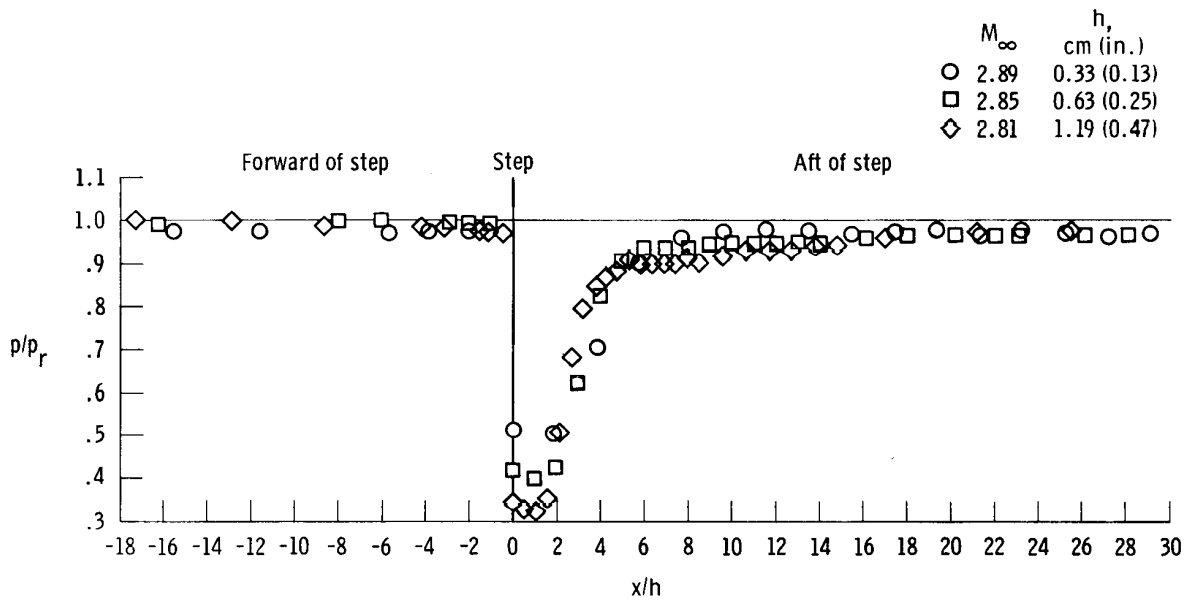

(c) $M_\infty \approx 2.80$.

Figure 12. Concluded.

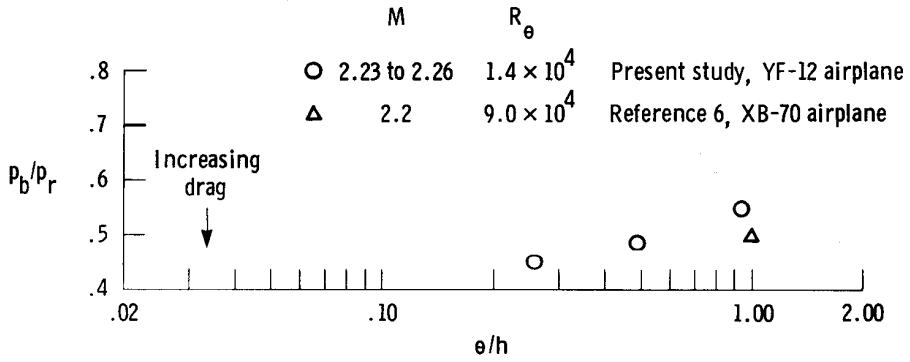

(a) $M \approx 2.20$.

Figure 13. Base pressure ratio as function of momentum thickness and step height.

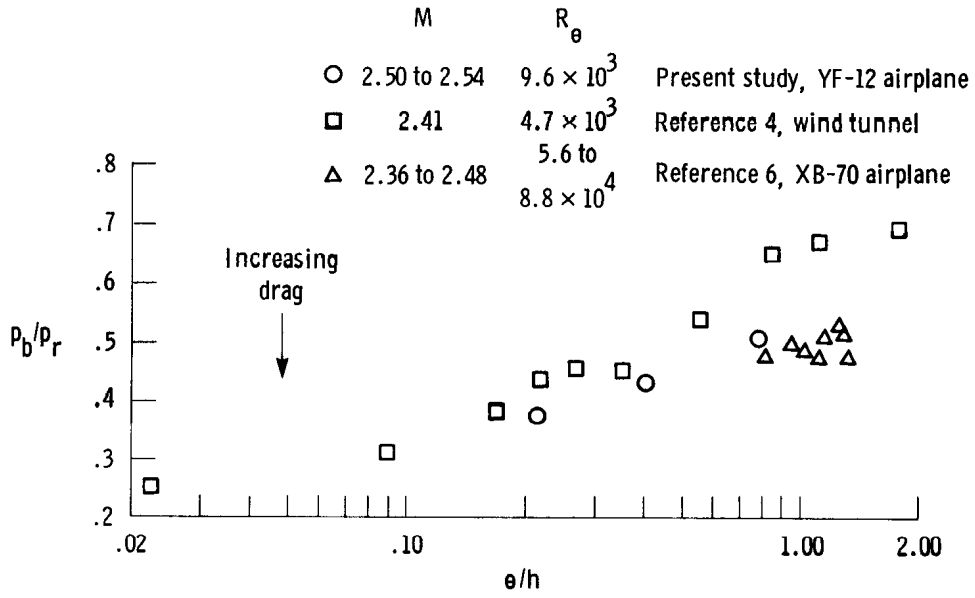

(b) $M \approx 2.50$.

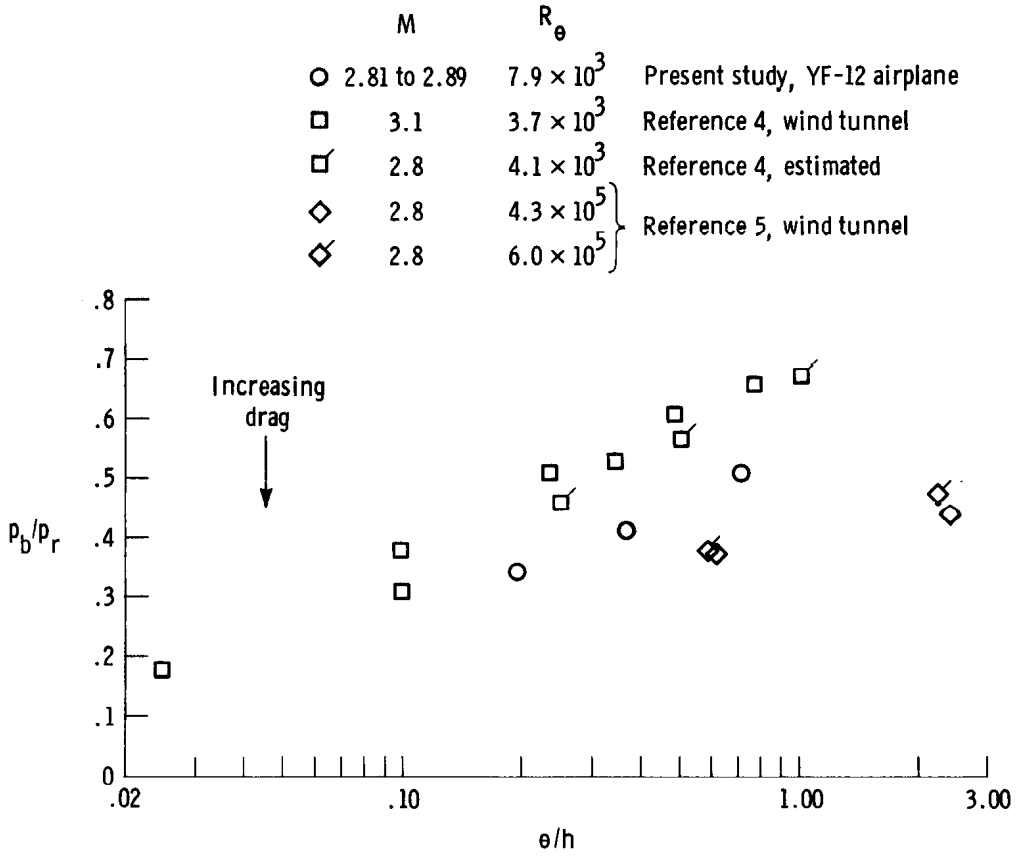

(c) $M \approx 2.80$.

Figure 13. Concluded.

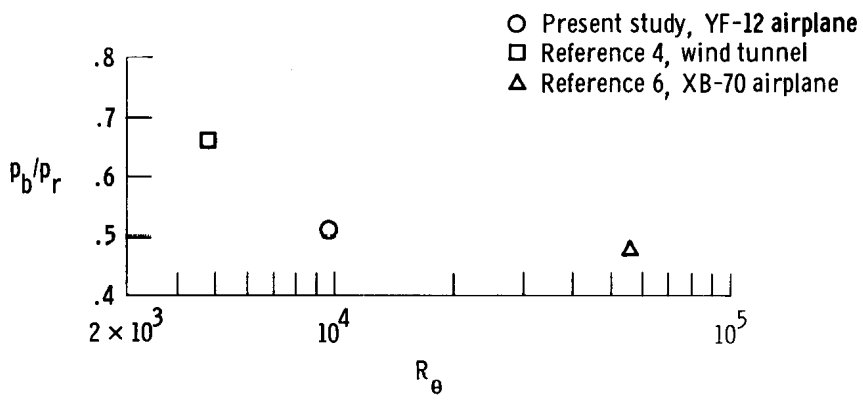

(a) $\theta/h = 0.8$; $M = 2.40$ *to* 2.50.

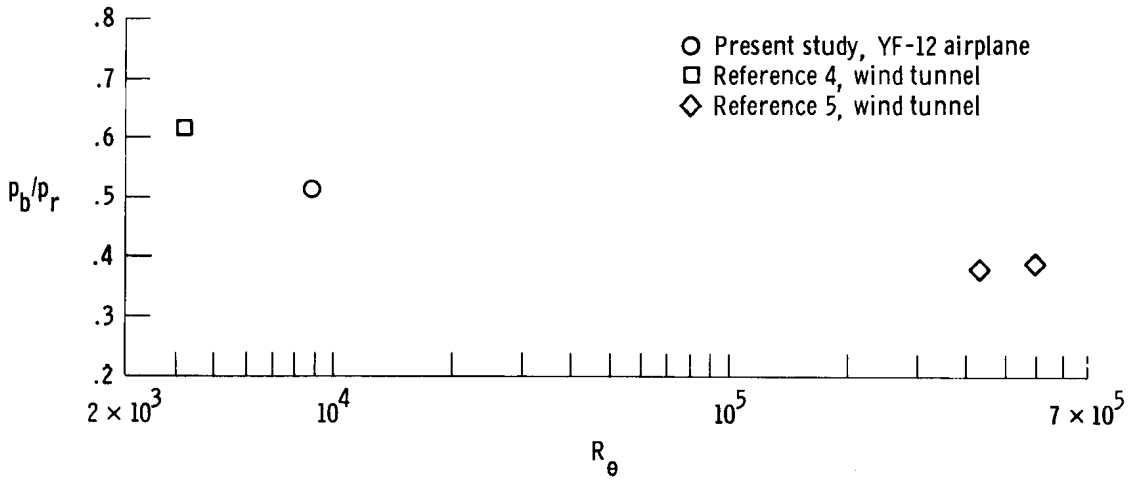

(b) $\theta/h = 0.7$; $M = 2.60$ *to* 2.80.

Figure 14. Base pressure ratio as function of Reynolds number based on momentum thickness.

1. Report No.	2. Government Accession No.	3. Recipient's Catalog No.
NASA TM-72855		

4. Title and Subtitle	5. Report Date
FLIGHT-MEASURED PRESSURE CHARACTERISTICS OF AFT-FACING STEPS IN HIGH REYNOLDS NUMBER FLOW AT MACH NUMBERS OF 2.20, 2.50, AND 2.80 AND COMPARISON WITH OTHER DATA	May 1978
	6. Performing Organization Code: H-956
7. Author(s): Sheryll Goecke Powers	8. Performing Organization Report No.
9. Performing Organization Name and Address: Dryden Flight Research Center, P.O. Box 273, Edwards, California 93523	10. Work Unit No.: 505-06-34
	11. Contract or Grant No.
12. Sponsoring Agency Name and Address: National Aeronautics and Space Administration, Washington, D.C. 20546	13. Type of Report and Period Covered: Technical Memorandum
	14. Sponsoring Agency Code

15. Supplementary Notes

16. Abstract

An experiment was conducted on the YF-12 airplane to determine the pressure characteristics associated with an aft-facing step in high Reynolds number flow for nominal Mach numbers of 2.20, 2.50, and 2.80. Base pressure coefficients were obtained for three step heights. The surface static pressures ahead of and behind the step were measured for the no-step condition and for each of the step heights. A boundary layer rake was used to determine the local boundary layer conditions.

The Reynolds number based on the length of flow ahead of the step was approximately 10^8, and the ratios of momentum thickness to step height ranged from 0.2 to 1.0. Base pressure coefficients from the present study are compared with other available data at similar Mach numbers and at ratios of momentum thickness to step height near 1.0. In addition, the data are compared with base pressure coefficients calculated by a semiempirical prediction method. The base pressure ratios are shown to be a function of Reynolds number based on momentum thickness. Profiles of the surface pressures ahead of and behind the step and the local boundary layer conditions are also presented.

17. Key Words (Suggested by Author(s))	18. Distribution Statement
Separated flow Base pressure	Unclassified - Unlimited Category: 02

19. Security Classif. (of this report)	20. Security Classif. (of this page)	21. No. of Pages	22. Price*
Unclassified	Unclassified	36	$3.75

For sale by the National Technical Information Service, Springfield, Virginia 22161

NASA-Langley, 1978